Volume 39 October 1974 Number 5

GEOPHYSICS

VELOCITY AND ATTENUATION OF SEISMIC WAVES IN TWO-PHASE MEDIA: PART I. THEORETICAL FORMULATIONS

GUY T. KUSTER* AND M. NAFI TOKSÖZ§

The propagation of seismic waves in two-phase media is treated theoretically to determine the elastic moduli of the composite medium given the properties, concentrations, and shapes of the inclusions and the matrix material. For long wavelengths the problem is formulated in terms of scattering phenomena in an approach similar to that of Ament (1959). The displacement fields, expanded in series, for waves scattered by an "effective" composite medium and individual inclusions are equated. The coefficients of the series expansions of the displacement fields provide a relationship between the elastic moduli of the effective medium and those of the matrix and inclusions. The expressions are derived for both solid and liquid inclusions in a solid matrix as well as for solid suspensions in a fluid matrix. Both spherical and oblate spheroidal inclusions are considered.

Some numerical calculations are carried out to demonstrate the effects of fluid inclusions of various shapes on the seismic velocities in rocks. It is found that the concentration, shapes, and properties of the inclusions are important parameters. A concentration of a fraction of one percent of thin (small aspect ratio) inclusions could affect the compressional and shear velocities by more than ten percent. For both sedimentary and igneous rock models, the calculations for "dry" (i.e., air-saturated) and water-saturated states indicate that the compressional velocities change significantly while the shear velocities change much less upon saturation with water.

INTRODUCTION

In the earth, where rocks are generally saturated or partly saturated with fluids, the seismic waves propagate through two-phase media. For theoretical treatment, a two-phase medium is defined as an aggregate of two homogeneous phases of different properties, where one phase (the matrix) is a continuum in which inclusions of the other phase are randomly embedded. If the two-phase medium is quasi-homogeneous, one could define a homogeneous medium (the effective medium) which is equivalent to the two-phase medium on a macroscopic scale. In this paper we will derive theoretical expressions for the effective properties of a two-phase medium for the propagation of elastic waves whose wavelengths are much longer than the size of an inclusion.

Theoretical treatments of the propagation of elastic waves in two-phase media (the dynamic problem) are relatively scarce. In a few studies on this subject (Ament, 1959; Mal and Knopoff,

Manuscript received by the Editor July 10, 1973; revised manuscript received February 22, 1974.

* Formerly MIT, Cambridge, Mass. Presently, Laboratoire de Detection et de Geophysique, Bretigny sur Orge, France.

§ MIT, Cambridge, Mass. 02139.

© 1974 Society of Exploration Geophysicists. All right reserved.

Downloaded 05/16/13 to 147.188.128.74. Redistribution subject to SEG license or copyright; see Terms of Use at http://library.seg.org/

Downloaded 05/16/13 to 147.188.128.74. Redistribution subject to SEG license or copyright; see Terms of Use at http://library.seg.org/

1967), the results were restricted to the case where the matrix is solid and the inclusions are spherical, much smaller than the wavelengths, and sufficiently far apart from each other so that interactions are negligible. Ament (1953) studied the case of rigid spheres in a viscous liquid matrix. Biot (1956a, b) treated the problem for porous rocks for both high- and low-frequency limits. His elegant formulations require the specification of a number of parameters before the effective medium properties can be computed. Chekin (1970) worked on the problem of wave propagation in rocks with cracks, but his formulations were for zero-width cracks.

The theoretical elastic behavior of two-phase media under static loading has been studied in detail (see Hashin, 1970, for a review). The results of these studies have been applied to seismic problems under the assumption that the conditions prevailing in the propagation of long wavelength waves can be approximated by those of static loading (Eshelby, 1957; Hashin, 1962; Hashin and Shtrikman, 1963; Wu, 1966; Walsh, 1969; Solomon, 1972; Dederichs and Zeller, 1973; Korringa, 1973; Zeller and Dederichs, 1973). The static approaches, although not exact formulations for the dynamic problem, have led to most useful results. As our comparisons will show, scattering phenomena and inertia effects (intrinsic features of the wave propagation generally omitted in static models) become of importance only in limited cases.

In this paper we follow the approach of Ament (1959) and formulate the problem in terms of scattering phenomena. We repeat his derivation for spherical inclusions embedded in a solid matrix, and we treat the additional cases of a fluid matrix and of spheroidal inclusions. All our models involve the assumptions that the wavelengths are much longer than the size of the inclusions and that multiple scattering effects are negligible.

THEORETICAL FORMULATION IN TERMS OF SCATTERING

Consider N inclusions randomly embedded within a finite region V_0 of an infinite matrix (Figure 1). Let an elastic wave be incident from infinity. We may write the displacement $\mathbf{u}(\mathbf{x})$ observed at a point $\mathbf{x}$ outside V_0 as

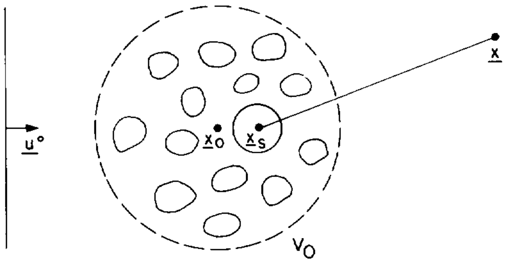

FIG. 1. Schematic diagram illustrating the scattering of a plane wave ($\mathbf{u}°$) by a representative sphere V_0 (dashed circle) of the effective medium. Individual inclusions are outlined by solid lines. The scattered fields are evaluated at point $\mathbf{x}$.

$$\mathbf{u}(\mathbf{x}) = \mathbf{u}^0(\mathbf{x}) + \sum_{s=1}^{N} \mathbf{u}^s(\mathbf{x}, \mathbf{x}_s), \tag{1}$$

where $\mathbf{u}^s(\mathbf{x}, \mathbf{x}_s)$ is the displacement observed at $\mathbf{x}$ due to the wave scattered by the sth inclusion located at $\mathbf{x}_s$ and where $\mathbf{u}^0(\mathbf{x})$ is the displacement due to the incident wave.

When examined on the scale of V_0, Figure 1 also represents a piece of a two-phase medium isolated in an infinite matrix. Assuming that the two-phase medium is homogeneous on the scale of V_0, we can define the properties of the effective medium to be the same as those of a homogeneous medium which, when confined to the volume V_0 and illuminated by the same incident wave $\mathbf{u}^0$, produces the same displacement field at the point $\mathbf{x}$ as the field generated by the N inclusions. We may write

$$\mathbf{u}(\mathbf{x}) = \mathbf{u}^0(\mathbf{x}) + \mathbf{u}^*(\mathbf{x}, \mathbf{x}_0), \tag{2}$$

where $\mathbf{u}^*(\mathbf{x}, \mathbf{x}_0)$ is the scattered displacement field observed at $\mathbf{x}$ due to the volume V_0 having effective properties and located at x_0.

Equating (1) and (2), we obtain the fundamental equation defining the effective medium

$$\mathbf{u}^*(\mathbf{x}, \mathbf{x}_0) = \sum_{s=1}^{N} \mathbf{u}^s(\mathbf{x}, \mathbf{x}_s). \tag{3}$$

If we assume that the two-phase medium is isotropic, the effective medium will also be isotropic, and we must take a sphere for the volume V_0 so that the scattered waves do not depend on the orientation of V_0 with respect to the incident field. Thus, from here on we shall call the volume V_0 the representative sphere.

In order to solve (3) for the effective properties

LIST OF SYMBOLS

A	amplitude of incident plane P-wave
A_{ijpq}	fourth order tensor
a	radius of spherical inclusion
B_n	coefficient in the series expansion of scattered P-waves
c	volume concentration of inclusions
c_{ijpq}	elastic tensor, matrix
c'_{ijpq}	elastic tensor, inclusion
e_{ij}	incident strain field
e^0_{ij}	strain field
G_{ki}	Green's function, matrix
$h_n^{(1)}$	spherical Hankel function, first kind
j_n	spherical Bessel function
K	matrix bulk modulus
K'	inclusion bulk modulus
K^*	effective bulk modulus
l_{ij}	direction cosine
N	number of inclusions in representative sphere
p	wavenumber, P-wave in matrix
p'	wavenumber, P-wave in inclusion
$P_n(\cos\theta)$	Legendre polynomial, order n
R	radius, representative sphere
s	wavenumber, S-wave in matrix
s'	wavenumber, S-wave in inclusion
T_{ijpq}	fourth order tensor, depending on matrix and inclusion properties
U_{ijpq}	fourth order tensor
$\mathbf{u}$	total displacement vector
$\mathbf{u}^0$	incident displacement vector
$\mathbf{u}^s$	scattered displacement vector for sth inclusion
$\mathbf{u}^*$	scattered displacement vector from representative sphere
$\Delta\mathbf{u}$	scattered displacement vector
u	radial displacement
u^j	radial displacement scattered from jth inclusion
u^*	radial displacement scattered from representative sphere
V	volume of an inclusion
V_0	volume of representative sphere
V_j	volume of jth inclusion in representative sphere
$\mathbf{v}$	displacement vector inside an inclusion
v	transverse displacement
v^j	transverse displacement scattered from jth inclusion
v^*	transverse displacement scattered from representative sphere
$\mathbf{x}$	point in the matrix
$\mathbf{x}_0$	center of representative sphere
$\mathbf{x}_s$	center of sth inclusion
α	aspect ratio of oblate spheroid
α^*	effective P-wave velocity
α_s^*	effective "static" P-wave velocity
β^*	effective S-wave velocity
λ	matrix Lamé's constant
λ'	inclusion Lamé's constant
μ	matrix shear modulus
μ'	inclusion shear modulus
μ^*	effective shear modulus
ρ	matrix density
ρ'	inclusion density
ρ^*	effective density
ρ_g^*	effective gravitational density
ξ	point inside an inclusion
ζ	center of an inclusion
ζ^0	center of representative sphere
η	viscosity
ω	angular frequency

exactly, a complete statistical description of the distribution of the inclusions is required. The wave scattered by each inclusion is a function of the wave incident on this particular inclusion, and this incident wave depends on the location of the other inclusions because of multiple scattering effects. The relative location of all inclusions must also be known for the calculation of the sum of all scattered waves. Such statistical information is not available for real two-phase media. Usually, only the relative volume fractions of the phases are known. In order to solve (3) with the limited information we have, we make two additional assumptions: (a) we assume that the observation point $\mathbf{x}$ is sufficiently far from the representative sphere so that we may take as a first approximation

$$\mathbf{x}_s \simeq \mathbf{x}_0, \qquad s = 1, N,$$

and (b) we assume that multiple scattering ef-

Downloaded 05/16/13 to 147.188.128.74. Redistribution subject to SEG license or copyright; see Terms of Use at http://library.seg.org/

Downloaded 05/16/13 to 147.188.128.74. Redistribution subject to SEG license or copyright; see Terms of Use at http://library.seg.org/

fects are negligible, which allows us to take the undisturbed incident field as the field incident on each inclusion within the representative sphere. The latter assumption restricts the validity of our results to small volume concentrations of inclusions or, in other words, to the case of noninteracting inclusions. The possibility of taking interactions into account by the use of self-consistent schemes is discussed elsewhere (Kuster, 1972).

With these approximations, the problem of finding the effective properties of a two-phase medium reduces to the estimation of the scattered displacement field due to an inclusion isolated in an infinite matrix, given a monochromatic incident wave of long wavelength.

Even this simplified problem is amenable to mathematical treatment only when the inclusion is of a regular shape, such as a sphere or a spheroid.

Scattering by spherical inclusions

Consider a homogeneous and isotropic sphere with elastic constants λ' and μ' and density ρ' embedded in a homogeneous and isotropic infinite matrix with elastic constants λ and μ and density ρ. Let a plane P-wave with displacement u_x be incident along the x-axis. Let

$$u_x = \frac{A}{ip} e^{i(px-\omega t)}, \tag{4}$$

where A is the amplitude, p the wavenumber, and ω the angular frequency. The presence of the sphere generates four additional waves: P- and S-waves inside the sphere and P- and S-waves scattered into the matrix. We formulate the problem in spherical coordinates with the origin at the center of the sphere (Figure 1). Because of the symmetries of the problem we need not consider the azimuthal dependence. Following Yamakawa (1962), we express the radial and transverse displacements u and v corresponding to each wave in an infinite series of spherical Bessel functions and Legendre polynomials. Thus the incident P-wave components are:

$$\begin{aligned} u_0 &= -\frac{A}{p^2}\sum_{n=0}^{\infty}(2n+1)i^n\frac{d}{dr}j_n(pr)P_n(\cos\theta),\\ v_0 &= -\frac{A}{p^2}\sum_{n=1}^{\infty}(2n+1)i^n\frac{j_n(pr)}{r}\frac{d}{d\theta}P_n(\cos\theta). \end{aligned} \tag{5}$$

The scattered P-waves are

$$\begin{aligned} u_1 &= -\frac{1}{p^2}\sum_{n=0}^{\infty}B_n\frac{d}{dr}h_n^{(1)}(pr)P_n(\cos\theta),\\ v_1 &= -\frac{1}{p^2}\sum_{n=1}^{\infty}B_n\frac{h_n^{(1)}(pr)}{r}\frac{d}{d\theta}P_n(\cos\theta). \end{aligned} \tag{6}$$

The scattered S-waves are

$$\begin{aligned} u_2 &= -\frac{1}{s^2}\sum_{n=1}^{\infty}C_n n(n+1)\frac{h_n^{(1)}(sr)}{r}P_n(\cos\theta),\\ v_2 &= -\frac{1}{s^2}\sum_{n=1}^{\infty}\frac{C_n}{r}\frac{d}{dr}\left[rh_n^{(1)}(sr)\right]\frac{d}{d\theta}P_n(\cos\theta). \end{aligned} \tag{7}$$

The P-waves in the sphere are

$$\begin{aligned} u_3 &= -\frac{1}{p'^2}\sum_{n=0}^{\infty}D_n\frac{d}{dr}j_n(p'r)P_n(\cos\theta),\\ v_3 &= -\frac{1}{p'^2}\sum_{n=1}^{\infty}D_n\frac{j_n(p'r)}{r}\frac{d}{d\theta}P_n(\cos\theta). \end{aligned} \tag{8}$$

The S-waves in the sphere are

$$\begin{aligned} u_4 &= -\frac{1}{s'^2}\sum_{n=1}^{\infty}E_n n(n+1)\frac{j_n(s'r)}{r}P_n(\cos\theta),\\ v_4 &= -\frac{1}{s'^2}\sum_{n=1}^{\infty}\frac{E_n}{r}\frac{d}{dr}\left[rj_n(s'r)\right]\frac{d}{d\theta}P_n(\cos\theta). \end{aligned} \tag{9}$$

The $e^{-i\omega t}$ time dependence is omitted throughout for brevity and p and s denote the wavenumbers of P- and S-waves in matrix material; p' and s' are wavenumbers in the inclusion. $P_n(\cos\theta)$ is the Legendre polynomial of the nth order, $j_n(z)$ is the spherical Bessel function of the nth order and $h_n^{(1)}(z)$ is the spherical Hankel function of the first kind and the nth order. We must use $h_n^{(1)}(z)$ for waves traveling radially outward because we adopted an $e^{-i\omega t}$ time dependence. The coefficients in the series are determined from the boundary conditions on the surface of the sphere (continuity of displacements and normal stresses at $r=a$). The detailed calculation of the scattered waves is given in Appendix A in the case of interest to us where the wavelengths of *all* waves (incident as well as scattered and transmitted) are much longer than the radius of the sphere, and where the observation point is at a large distance from the sphere. With these approximations the scattered waves can be written as

$$u = -\frac{iA}{p}(pa)^3 \frac{e^{i(pr-\omega t)}}{pr} \cdot \left[Be_0 - Be_1 \cos\theta - \frac{Be_2}{4}(3\cos 2\theta + 1) \right],$$

$$v = -iA \frac{(sa)^3}{p} \frac{e^{i(sr-\omega t)}}{sr} \cdot \left[Be_1 \sin\theta + \frac{3s}{4p} Be_2 \sin 2\theta \right], \tag{10}$$

where

$$Be_0 = \frac{K - K'}{3K' + 4\mu},$$

$$Be_1 = \frac{\rho - \rho'}{3\rho}, \tag{11}$$

$$Be_2 = \frac{20}{3} \frac{\mu(\mu' - \mu)}{6\mu'(K + 2\mu) + \mu(9K + 8\mu)}.$$

The neglected terms are of order $(pa)^5$.

It was shown by Yamakawa (1962) that in the case of a spherical cavity the scattered waves can be obtained from equations (10) and (11) by letting K', μ', and ρ' vanish; and in the case of a fluid-filled cavity by letting μ' vanish. However, the solution for the case of a fluid matrix cannot be obtained by simply letting μ vanish. In this case, the scattered waves can be written as (see Appendix A for the detailed derivation)

$$u = -\frac{iA(pa)^3}{p} \frac{e^{i(pr-\omega t)}}{pr} \cdot \left[\overset{0}{Be_0} - \overset{0}{Be_1} \cos\theta \right], \tag{12}$$

where

$$\overset{0}{Be_0} = \frac{K - K'}{3K'},$$

$$\overset{0}{Be_1} = \frac{\rho - \rho'}{\rho + 2\rho'}. \tag{13}$$

The terms neglected are of order $(pa)^5$. This result holds whether the inclusion is solid or fluid.

The difference between the solid and fluid matrix cases resides essentially in the second term ($n = 1$). This term represents a single force source which expresses the change in inertia due to the replacement of matrix material by inclusion material. When the matrix is solid, the change in inertia arises only from the density difference between matrix and inclusion since there is no relative motion between the matrix and inclusion. But when the matrix is fluid, relative motion does occur (Lamb, 1932), and the inertia term is therefore modified.

A spheroidal inclusion

We wish to find the waves scattered by a spheroidal inclusion embedded in a solid matrix. We cannot follow the same procedure as for a spherical inclusion since the vector wave equation is not separable in spheroidal coordinates (Morse and Feshbach, 1953). Rather, we shall use an integral expression derived by Mal and Knopoff (1967) for the displacement due to the waves scattered by an inclusion of arbitrary shape isolated in an infinite matrix. Denoting the displacement field of the scattered waves observed at a point $\mathbf{x}$ in the matrix by $\Delta\mathbf{u}(\mathbf{x})$, the displacement field of the wave at a point $\boldsymbol{\xi}$ inside the inclusion by $\mathbf{v}(\boldsymbol{\xi})$, the kth component of the Green's function due to a point force acting in the ith direction at a point $\mathbf{y}$ in the infinite matrix by $G_{ki}(\mathbf{x}, \mathbf{y})$ and the elastic tensor in the matrix by c_{ijpq}, we have

$$\Delta u_k(\mathbf{x}) = \int_V \left\{ \omega^2(\rho' - \rho) v_i(\boldsymbol{\xi}) G_{ki}(\mathbf{x}, \boldsymbol{\xi}) - (c'_{ijpq} - c_{ijpq}) \frac{\partial v_p}{\partial \xi_q} \frac{\partial G_{ki}}{\partial \xi_j}(\mathbf{x}, \boldsymbol{\xi}) \right\} d\boldsymbol{\xi}. \tag{14}$$

The summation convention is used, and for brevity we omit the assumed $e^{i\omega t}$ time dependence. The integral is taken over the volume V of the inclusion. If the displacement and strain inside the inclusion can be estimated in terms of the incident field, we can obtain the desired expression for the scattered field.

The estimation of the displacement and strain inside the inclusion is given in Appendix B under the assumptions that the matrix is solid, that the inclusion is spheroidal, and that the wavelengths are much longer than the inclusion. For an observation point located at a large distance from the inclusion, the displacement field scattered by a spheroid of arbitrary orientation can be written as

Downloaded 05/16/13 to 147.188.128.74. Redistribution subject to SEG license or copyright; see Terms of Use at http://library.seg.org/

$$\Delta u_k(\mathbf{x}, \boldsymbol{\zeta}) = V\left[\omega^2(\rho'-\rho)\overset{0}{u_i}(\boldsymbol{\zeta})G_{ki}(\mathbf{x}, \boldsymbol{\zeta}) - [(\lambda'-\lambda)U_{pprs}\delta_{ij} + 2(\mu'-\mu)U_{ijrs}]\overset{0}{e_{rs}} \frac{\partial G_{ki}}{\partial \zeta_j}(\mathbf{x}, \boldsymbol{\zeta})\right]. \quad (15)$$

The corresponding expression for a spherical inclusion was derived by Mal and Knopoff (1967):

$$\Delta u_k(\mathbf{x}, \boldsymbol{\zeta}) = V\left[\omega^2(\rho' - \rho)\overset{0}{u_i}(\boldsymbol{\zeta})G_{ki}(\mathbf{x}, \boldsymbol{\zeta}) - \{[P(K' - K) - \tfrac{2}{3}(\mu' - \mu)Q]\delta_{ij}\overset{0}{e_{pp}} + 2Q(\mu' - \mu)\overset{0}{e_{ij}}\} \frac{\partial G_{ki}}{\partial \zeta_j}(\mathbf{x}, \boldsymbol{\zeta})\right]. \quad (16)$$

THE EFFECTIVE PROPERTIES OF TWO-PHASE MEDIA

In order to obtain the effective properties of two-phase media we now use equation (3) and the expressions derived above for the scattered waves.

Spherical inclusions

Consider N spherical inclusions embedded in an infinite solid matrix and confined to the representative sphere of radius R. Let a plane P-wave of amplitude A be incident from infinity. At a distant observation point, with the assumptions listed in the previous section, the waves scattered by the representative sphere are given by an expression of the type of equation (10):

$$u^* = -\frac{iA(pR)^3}{p}\frac{e^{i(pr-\omega t)}}{pr}\left[Be_0^* - Be_1^*\cos\theta - \frac{Be_2^*}{4}(3\cos 2\theta + 1)\right], \quad (17)$$

$$v^* = -\frac{iA(sR)^3}{p}\frac{e^{i(sr-\omega t)}}{sr} \cdot \left[Be_1^*\sin\theta + \frac{3s}{4p}Be_2^*\sin 2\theta\right],$$

where

$$Be_0^* = \frac{K - K^*}{3K^* + 4\mu}, \qquad Be_1^* = \frac{\rho - \rho^*}{3\rho},$$

$$Be_2^* = \frac{20}{3}\frac{\mu(\mu^* - \mu)}{6\mu^*(K + 2\mu) + \mu(9K + 8\mu)}.$$

Assuming that multiple scattering effects are negligible so that the wave incident on each inclusion is the original plane P-wave, we can also write the scattered waves at the observation point as the sum of the waves scattered by each inclusion. Thus we also have

$$\sum_{j=1}^{N} u^j = -\frac{iA}{p}\sum_{j=1}^{N}(pa_j)^3\frac{e^{i(pr-\omega t)}}{pr} \cdot \left[Be_0 - Be_1\cos\theta - \frac{Be_2}{4}(3\cos 2\theta + 1)\right],$$

$$\sum_{j=1}^{N} v^j = -\frac{iA}{p}\sum_{j=1}^{N}(sa_j)^3\frac{e^{i(sr-\omega t)}}{sr} \cdot \left[Be_1\sin\theta + \frac{3s}{4p}Be_2\sin 2\theta\right], \quad (18)$$

where

$$Be_0 = \frac{K - K'}{3K' + 4\mu}, \qquad Be_1 = \frac{\rho - \rho'}{3\rho},$$

$$Be_2 = \frac{20}{3}\frac{\mu(\mu' - \mu)}{6\mu'(K + 2\mu) + \mu(9K + 8\mu)}.$$

Because of our definition of the effective medium by equation (3), we obtain the effective properties by equating (17) and (18). Since the equality must hold independently of the angle θ, the coefficients of the corresponding angular terms must be equal. Thus, we obtain the composition laws for the effective elastic constants and density

$$\frac{K^* - K}{3K^* + 4\mu} = c\frac{K' - K}{3K' + 4\mu}, \quad (19)$$

$$\rho^* - \rho = c(\rho' - \rho), \quad (20)$$

$$\frac{\mu^* - \mu}{6\mu^*(K + 2\mu) + \mu(9K + 8\mu)} = \frac{c(\mu' - \mu)}{6\mu'(K + 2\mu) + \mu(9K + 8\mu)}, \quad (21)$$

where c, the volume concentration of inclusions, is given by

$$c = \frac{1}{R^3}\sum_{j=1}^{N} a_j^3. \quad (22)$$

Downloaded 05/16/13 to 147.188.128.74. Redistribution subject to SEG license or copyright; see Terms of Use at http://library.seg.org/

Downloaded 05/16/13 to 147.188.128.74. Redistribution subject to SEG license or copyright; see Terms of Use at http://library.seg.org/

The corresponding effective P- and S-wave velocities are

$$\alpha^* = \left[\frac{K^* + 4\mu^*/3}{\rho^*}\right]^{1/2}, \quad \beta^* = \left[\frac{\mu^*}{\rho^*}\right]^{1/2}. \tag{23}$$

The effective properties derived here were obtained earlier by Ament (1959). The assumptions involved in their derivation are: (a) the matrix is solid, (b) the inclusions are spherical, (c) the wavelengths of all waves are much longer than the inclusion radius, and (d) multiple scattering effects can be neglected. Because of the latter assumption, the validity of this model is limited to two-phase media where the concentration of inclusions is small. Also, the effective elastic moduli in this model reduce to those found by Mal and Knopoff (1967) if the concentration of inclusions is much smaller than unity. The Mal and Knopoff model is probably valid for lower concentrations than the model derived above.

In the case of a nonviscous fluid matrix, one must use (12) as the expression of the waves scattered both by the representative sphere and by each solid spherical inclusion. Introducing (12) with the appropriate starred or primed variables in (3), identifying the coefficients of the corresponding angular terms, and using (22), we obtain the following composition laws

$$\frac{K - K^*}{K^*} = c\,\frac{K - K'}{K'}, \tag{24}$$

$$\frac{\rho - \rho^*}{\rho + 2\rho^*} = c\,\frac{\rho - \rho'}{\rho + 2\rho'}. \tag{25}$$

The effective shear modulus vanishes because a two-phase medium cannot sustain any shear unless there is a solid continuum. The effective P-wave velocity is given by

$$\alpha^* = \sqrt{K^*/\rho^*}. \tag{26}$$

It is of interest to note that the effective P-wave velocity is independent of the shear modulus of the inclusions. Thus our result is identical with that obtained by Ament (1953) for suspensions of perfectly rigid spheres in a nonviscous fluid matrix. It must be emphasized that ρ^* is an effective inertial density since (25) is a relation between inertia terms. In the case of a fluid matrix, where relative motion between the inclusion and matrix can occur, the effective inertial density is different from the effective gravitational density, which is given by

$$\overset{*}{\rho_g} = \rho(1 - c) + \rho' c. \tag{27}$$

Because of this difference resulting from inertia effects, the static and dynamic velocity formulas differ. In the static problem the effective bulk modulus is given by the Reuss average, which is in fact equation (24), but one would have taken ρ_g^* as the density of the medium, and thus the effective "static" P-wave velocity would have been

$$\overset{*}{\alpha_g} = \sqrt{\frac{K^*}{\rho_g^*}}. \tag{28}$$

The static velocity calculated with equation (28) can be significantly different from the effective P-wave velocity given by equation (26) when the density contrast between matrix and inclusion materials is large.

Spheroidal inclusions

We again use equation (3) to obtain the effective properties. The field scattered by the representative sphere centered at $\boldsymbol{\zeta}^0$ is given by

$$\begin{aligned}\Delta \overset{*}{u}_k(\mathbf{x}, \overset{0}{\boldsymbol{\zeta}}) &= V_0\Bigg\{\omega^2(\overset{*}{\rho} - \rho)\overset{0}{u}_i(\overset{0}{\boldsymbol{\zeta}})G_{ki}(\mathbf{x}, \overset{0}{\boldsymbol{\zeta}}) \\ &\quad - \Bigg[\overset{*}{P}(\overset{*}{K} - K)\delta_{ij}\overset{0}{e}_{pp} + 2\overset{*}{Q}(\overset{*}{\mu} - \mu) \\ &\quad \cdot \left(\overset{0}{e}_{ij} - \delta_{ij}\frac{\overset{0}{e}_{pp}}{3}\right)\Bigg]\frac{\partial G_{ki}}{\partial \zeta_j^0}(\mathbf{x}, \overset{0}{\boldsymbol{\zeta}})\Bigg\},\end{aligned} \tag{29}$$

where P^* and Q^* are obtained from (B-4) by letting all primed variables become starred variables. In order to evaluate the sum of the fields scattered by all spheroids within the representative sphere, we assume that (a) multiple scattering effects are negligible so that the field incident on each spheroid is also $\mathbf{u}^0$, (b) the orientation of the spheroids is uniform over all directions so that the two-phase medium is isotropic on a large

Downloaded 05/16/13 to 147.188.128.74. Redistribution subject to SEG license or copyright; see Terms of Use at http://library.seg.org/

scale, (c) the distribution function of the orientation can be represented by a continuous function although there is a finite number of spheroids in the representative sphere, and (d) all inclusions are approximately located at $\boldsymbol{\zeta}^0$. Then using (15), we may write the sum of the fields scattered by all inclusions as

$$\sum_{n=1}^{N} \Delta \overset{n}{u}_k(\mathbf{x}, \overset{0}{\boldsymbol{\zeta}}) = \sum_{n=1}^{N} V_n \Big\{ \omega^2 (\rho' - \rho) \overset{0}{u}_i(\overset{0}{\boldsymbol{\zeta}}) G_{ki}(\mathbf{x}, \overset{0}{\boldsymbol{\zeta}}) - \left[(\lambda' - \lambda)\delta_{ij} A_{pprs} + 2(\mu' - \mu) A_{ijrs} \right] \cdot \overset{0}{e}_{rs} \frac{\partial G_{ki}}{\partial \zeta_j^0}(\mathbf{x}, \overset{0}{\boldsymbol{\zeta}}) \Big\}, \tag{30}$$

where V_n is the volume of the nth inclusion, N is the number of inclusions in the representative sphere, and

$$A_{ijkl} = \frac{1}{4\pi} \int_0^\pi \sin\theta d\theta \int_0^{2\pi} U_{ijkl} d\psi. \tag{31}$$

Equating (29) and (30), and setting

$$\frac{1}{V_0} \sum_{n=1}^{N} V_n = c, \tag{32}$$

we obtain

$$\omega^2 G_{ki}(\mathbf{x}, \boldsymbol{\zeta}) \overset{0}{u}_i(\boldsymbol{\zeta}) \left[(\rho^* - \rho) - c(\rho' - \rho) \right] - \Big\{ \delta_{ij} \overset{0}{e}_{pp} P^* (K^* - K) + 2Q^* (\mu^* - \mu) \cdot \left(\overset{0}{e}_{ij} - \delta_{ij} \frac{\overset{0}{e}_{pp}}{3} \right) - c(\lambda' - \lambda) \delta_{ij} A_{pprs} \overset{0}{e}_{rs} - 2c(\mu' - \mu) A_{ijrs} \overset{0}{e}_{rs} \Big\} \frac{\partial G_{ki}}{\partial \zeta_j} = 0. \tag{33}$$

Requiring that both terms are identically zero, we have the density composition law from the first term,

$$\rho^* = \rho(1 - c) + \rho' c, \tag{34}$$

and the composition law for the elastic constants from the second term. If the incident field is purely dilatational, that is

$$\overset{0}{e}_{ij} = e\delta_{ij}, \tag{35}$$

the second term becomes

$$3eP^*(K^* - K) G_{ki,i} = ceG_{ki,j} \left[\delta_{ij} (\lambda' - \lambda) A_{ppnn} + 2(\mu' - \mu) A_{ijnn} \right]. \tag{36}$$

From the symmetries of the tensor $T_{\alpha\beta\gamma\delta}$ (see Appendix B) and the integration in (31), we find that

$$\begin{aligned} A_{ppnn} &= \tfrac{1}{3} T_{iijj}, \\ A_{ijnn} &= 0 \qquad \text{if } i \neq j. \end{aligned} \tag{37}$$

Combining (36) and (37) we obtain the composition law for the bulk modulus,

$$\frac{K^* - K}{3K^* + 4\mu} = c \frac{K' - K}{3K + 4\mu} \frac{1}{3} T_{iijj}. \tag{38}$$

The composition law for the shear modulus is obtained in a very similar way by taking the incident field as

$$\overset{0}{e}_{ij} = \begin{cases} 0 & i = j \\ e & i \neq j. \end{cases} \tag{39}$$

Thus, we have

$$\frac{\mu^* - \mu}{6\mu^*(K + 2\mu) + \mu(9K + 8\mu)} = \frac{c(\mu' - \mu)}{25\mu(3K + 4\mu)} \left[T_{ijij} - \tfrac{1}{3} T_{iijj} \right]. \tag{40}$$

The scalars T_{iijj} and T_{ijij} are functions of the shape of the spheroid. They are given in Appendix B.

The essential result here is that the effective elastic moduli depend not only on the concentration but also on the shape of the inclusions (i.e., aspect ratio). This conclusion is in agreement with experimental data on porous rocks (Nur and Simmons, 1969) and with other theoretical formulations (Eshelby, 1957; Wu, 1966; Walsh, 1969). It is important to note that our assumption of noninteraction among the spheroids is violated when the ratio c/α is larger than 1 (Solomon, 1971) since the inclusions are then overlapping, at least partially.

In the above formulation, the results were for spheroids all having the same aspect ratio. These results can be easily extended to cover the case of a discrete spectrum of aspect ratios. When the concentration for each aspect ratio $c(\alpha_m)$ is known, the effective bulk modulus is given by

$$\frac{K^* - K}{3K^* + 4\mu} = \frac{K' - K}{3K + 4\mu} \sum_{m=1}^{M} c(\alpha_m)\tfrac{1}{3}T_{iijj}(\alpha_m). \tag{41}$$

Of course, the noninteraction assumption must still be valid, and it can be expressed as

$$\sum_{m=1}^{M} \frac{c(\alpha_m)}{\alpha_m} < 1. \tag{42}$$

We can compare our results (38) and (40) with those obtained by Walsh (1969) for a two-phase medium with noninteracting spheroidal inclusions.

$$\begin{aligned} K^* - K &= \frac{c}{3} T_{iijj}(K' - K) \\ \mu^* - \mu &= \frac{c}{5}(\mu' - \mu)(T_{ijij} - \tfrac{1}{3}T_{iijj}). \end{aligned} \tag{43}$$

To compare these with our results, we rewrite (38) and (40) in a slightly different form,

$$\begin{aligned} K^* - K &= \frac{c}{3}(K' - K)T_{iijj}\frac{3K^* + 4\mu}{3K + 4\mu}, \\ \mu^* - \mu &= \frac{c}{5}(\mu' - \mu)\left(T_{ijij} - \frac{T_{iijj}}{3}\right) \\ &\quad \cdot \frac{6\mu^*(K + 2\mu) + \mu(9K + 8\mu)}{5\mu(3K + 4\mu)}. \end{aligned} \tag{44}$$

It is clear that our results and those of Walsh differ somewhat. They are similar if the effective medium and the matrix are not too different. This may be the case if the concentration of inclusions and/or the elastic moduli contrast between inclusion and matrix materials is small. Now if the effective moduli derived for spheroidal inclusions are specialized to the limiting case of spheres, where

$$\tfrac{1}{3}T_{iijj} = \frac{3K + 4\mu}{3K' + 4\mu} \quad \text{and}$$

$$T_{ijij} - \tfrac{1}{3}T_{iijj} = \frac{25\mu(3K + 4\mu)}{6\mu'(K + 2\mu) + \mu(9K + 8\mu)}, \tag{45}$$

the results of Walsh reduce to those of Mal and Knopoff; our results in (44) become (19) and (21). Thus, at least in the case of spherical inclusions, our results are probably valid over a wider range of concentration than those of Walsh (1969).

NUMERICAL RESULTS AND DISCUSSION

To demonstrate the effects of the inclusions on the effective moduli and velocities of a two-phase medium we made a series of numerical calculations. For these calculations we assumed a solid matrix and inclusions of different shapes and properties which represent both dry and water-saturated rocks. The matrix parameters were chosen to represent those of the matrix of an average sandstone or quartz-rich crystalline rock: $K = 0.44$ Mb, $\mu = 0.37$ Mb, $\rho = 2.70$ gm/cc (Birch, 1966). For the "saturated" case we used water inclusions with the properties: $K' = 0.022$ Mb, $\mu' = 0$, and $\rho' = 1.00$ gm/cc. In the case of the "dry" state, it was assumed that the pores were filled with air at atmospheric pressure (bulk modulus $K' = 1.5$ bars).

With these input parameters, two separate types of calculations were carried out. The first set of calculations shows the effect of each pore type. For this we specified the pore shape and calculated the moduli and velocities of the composite medium as a function of pore concentration for both the saturated and dry states. The results are shown in Figures 2a, b.

The four aspect ratios chosen are $\alpha = 1.0$ (spherical pores) and $\alpha = 10^{-1}$, 10^{-2}, 10^{-4}, representing oblate spheroidal pores of different shapes ranging all the way to fine cracks. For ellipsoidal pores, the concentrations were varied from $c = 0$ to $c = \alpha$, the optimum limit specified by the noninteraction assumption [equation (42)]. The densities were computed using equation (27).

The four examples shown in Figures 2a, b demonstrate the effects of inclusion concentrations and shapes on the effective moduli and velocities. In all cases the moduli (K^*, μ^*) and the velocities decrease with increasing concentration of inclusions. For a given concentration

Downloaded 05/16/13 to 147.188.128.74. Redistribution subject to SEG license or copyright; see Terms of Use at http://library.seg.org/

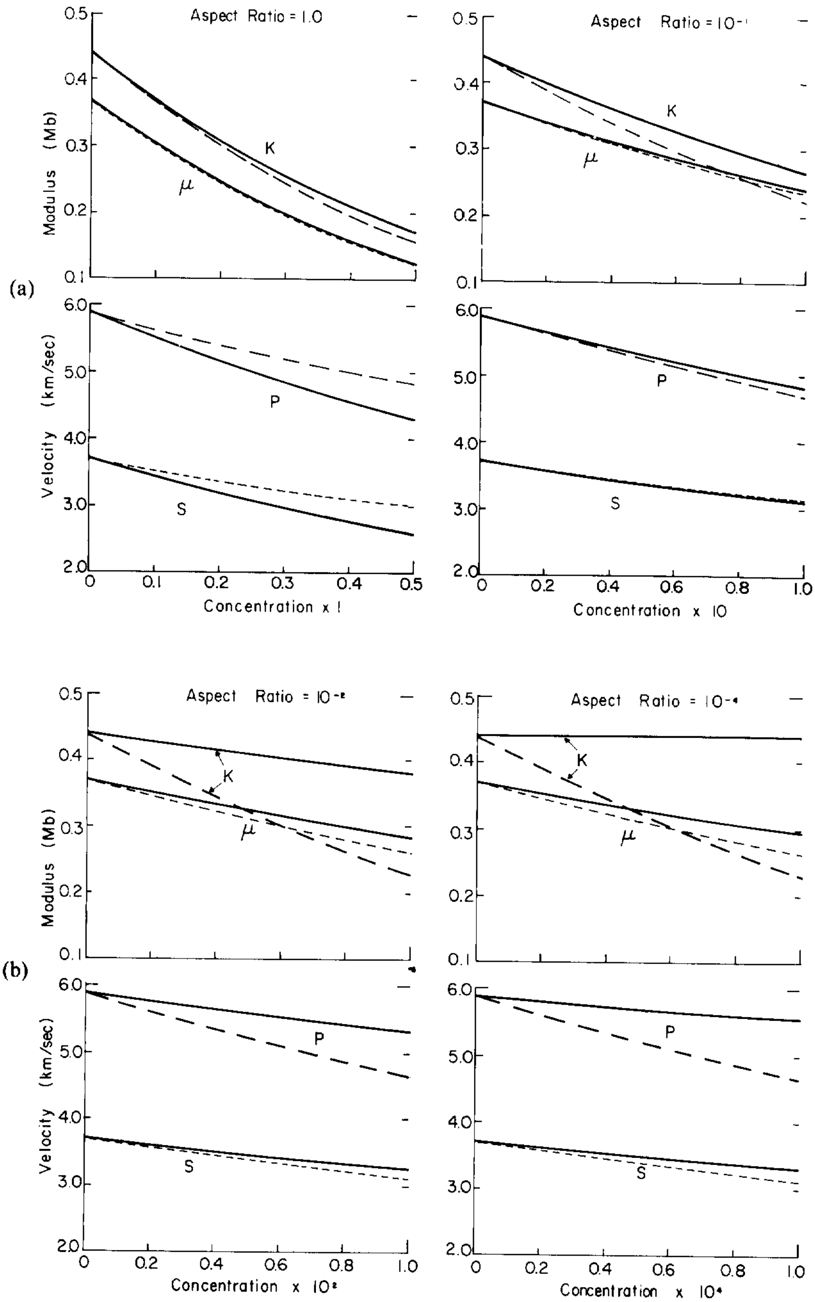

FIG. 2a, b. Elastic moduli (K, μ) and the compressional (P) and shear (S) velocities in a composite medium as a function of volume concentration of inclusions. The solid curves are the water-saturated and the dashed curves are the air-saturated ("dry") cases. The four sets of diagrams demonstrate the effects of inclusion shape specified by the aspect ratio. $\alpha=1.0$ corresponds to spherical inclusions; $\alpha=10^{-4}$ represents very flat oblate spheroidal inclusions modeling fine cracks or grain boundaries. Note the different multipliers in the concentration scale. The matrix moduli and velocities can be read at $c=0$. Matrix density $\rho=2.70$ gm/cc. The inclusion properties for water are $K'=22$ kb, $\mu'=0$, and $\rho'=1.00$ gm/cc; for air they are $K'=1.5$ bars, $\mu'=0$, and $\rho'=0.00$.

Downloaded 05/16/13 to 147.188.128.74. Redistribution subject to SEG license or copyright; see Terms of Use at http://library.seg.org/

the flatter inclusions have greater effect than the rounder inclusions. Even a very low concentration (i.e., 0.01 percent) of thin inclusions could decrease the velocities in the composite medium by as much as 10 percent or more.

The comparison of the moduli for the water-saturated and dry states reveals some important effects. At a given concentration of pores, the change from water-saturated to the air-saturated (dry) state produces a relative change in bulk modulus which is greater than the corresponding change in shear modulus. This is true regardless of the pore shape. For flat pores, the changes in both moduli are pronounced; for spherical pores, only the change in the bulk modulus is apparent.

The effects of water or gas saturation on compressional and shear velocities strongly depend on pore shapes as illustrated in Figures 2a, b. For spherical pores the velocities increase when one goes from the water-saturated to dry state. This is because the effect of density change in the composite medium is greater than the effect of changes in the moduli. Thus velocities increase in a change from wet to dry state while bulk and shear moduli are decreasing, because of the greater decrease in effective densities (equation 23). For intermediate shape pores, such as those with aspect ratio of about $\alpha=0.1$, the velocities in the dry and water-saturated states are about the same. For very thin pores and cracks, both P- and S-velocities are lower in the dry state than in the water-saturated case, although the decrease is much more pronounced in the case of P-waves. In these cases, the density changes are negligibly small; velocities in the two states are controlled by the effective moduli.

In a typical rock the pores are likely to have a spectrum of shapes. Equidimensional pores in sedimentary rocks can be approximated by spheres while grain boundary spaces can be approximated by flat cracks (low aspect ratio spheroids) as shown by electron microscope studies (Timur et al, 1971). To study the effects of saturation in rocks, a second set of calculations was carried out for models of a sedimentary rock (sandstone) and a crystalline rock with representative porosities: 14.2 percent for the sedimentary and 0.4 percent for the crystalline rock. The matrix model and the properties of the fluids (water and air) were the same as before. A spectrum of pore shapes was used in each case. For the sedimentary model the majority of pores (12 percent concentration) were assumed to be spherical pores; the remainder had smaller aspect ratios. These are listed in Table 1. For the crystalline model the majority of the pores were taken

Table 1. Theoretical elastic moduli and seismic velocities for examples of a sedimentary and a crystalline rock model in "dry" and "water-saturated" state. (In "dry" state the rock is saturated with air.)

PORE STRUCTURE USED FOR CALCULATIONS

Sedimentary model		Crystalline model	
Concentration (percent)	Aspect ratio	Concentration (percent)	Aspect ratio
12	1 (sphere)	0.01	1
2	10^{-1}	0.15	10^{-1}
1.	10^{-2}	0.20	10^{-2}
0.2×10^{-1}	10^{-3}	0.05	10^{-3}
0.1×10^{-2}	10^{-4}	0.10×10^{-3}	10^{-5}

CALCULATED MODULI AND VELOCITIES

	K (Mb)	μ (Mb)	ρ (gm/cc)	V_p (km/sec)	V_s (km/sec)
Matrix Properties	0.440	0.370	2.70	5.88	3.70
Sedimentary Model					
Water-saturated	0.276	0.186	2.44	4.62	2.75
"Dry" (air-saturated)	0.107	0.163	2.30	3.76	2.67
Crystalline Model					
Water-saturated	0.420	0.303	2.693	5:53	3.35
"Dry" (air-saturated)	0.260	2.280	2.690	4.85	3.23

Downloaded 05/16/13 to 147.188.128.74. Redistribution subject to SEG license or copyright; see Terms of Use at http://library.seg.org/

Downloaded 05/16/13 to 147.188.128.74. Redistribution subject to SEG license or copyright; see Terms of Use at http://library.seg.org/

to be thin cracks as indicated by the thin section photographs (Timur et al, 1971; Brace et al, 1972).

The calculated moduli and velocities are listed in Table 1. In all cases, calculations were carried out for the standard 1 atm pressure. The differences in moduli and velocities between the water-saturated and dry states are very significant. For the sedimentary rock model, the water-saturated compressional velocity is about 22 percent greater than the dry state velocity. The shear velocity difference is about 3 percent. For the crystalline rock model, although the total porosity is only 0.4 percent, the increase of compressional velocity upon water saturation is about 15 percent while the change in shear velocity is about 4 percent. Velocity changes of this nature have been observed in the laboratory for dry and saturated granites (Nur and Simmons, 1969).

These two sets of examples demonstrate the relative importance of the pore shapes and the compressibility and density of saturating fluids in determining the velocities in rocks. If pore shapes can be specified on the basis of laboratory measurements, then the nature of saturating fluids could be determined from P- and S-wave velocities.

The attenuation of elastic waves in two-phase media can be computed using the formulations given in this paper by assuming the moduli (K, μ) are complex. This is discussed in detail in the second paper (Kuster and Toksöz, this issue) along with experimental results.

ACKNOWLEDGMENTS

This research was supported by American Petroleum Institute Research Project 129 and the Advanced Research Projects Agency of the Dept. of Defense, and was monitored by the Air Force Office of Scientific Research under Contract no. F44620-71-C-0049. During part of this study, Guy Kuster was the recipient of a Chevron Oil Co. graduate fellowship.

We are grateful to our colleagues Drs. K. Aki, S. Solomon, J. Walsh, and D. Weidner for many beneficial discussions during the course of this work. We benefited greatly from the comments and suggestions of Drs. A. Timur, D. Thomson, J. Korringa, and R. Runge of Chevron Oil Field Research Co.

REFERENCES

Ament, W. S., 1953, Sound propagation in gross mixtures: J. Acoust. Soc. Am., v. 25, p. 638–641.

——— 1959, Wave propagation in suspensions: U.S. Naval Res. Lab., Rep. No. 5307.

Biot, M. A., 1956a, Theory of propagation of elastic waves in a fluid saturated porous solid: I. Low frequency range: J. Acoust. Soc. Am., v. 28, p. 168–178.

——— 1956b, Theory of propagation of elastic waves in a fluid saturated porous solid: II. Higher frequency range: J. Acoust. Soc. Am., v. 28, p. 179–191.

Birch, F., 1966, Compressibility; elastic constants, *in* Handbook of physical constants: S. P. Clark, ed., GSA, Mem. 97, p. 97–173.

Brace, W. B., 1972, Cracks and pores: A closer look: Science, v. 178, p. 162–164.

Chekin, B. S., 1970, Effective parameters of an elastic medium with randomly distributed fractures: Izv., Earth Phys. (English transl.), p. 619–623.

Dederichs, P. H., and Zeller, R., 1973, Variational treatment of the elastic constants of disordered materials: Z. Physik, v. 259, p. 103–116.

Eshelby, J. D., 1957. The determination of the elastic field of an ellipsoidal inclusion, and related problems: Proc. Roy. Soc. London, ser. A, v. 241, p. 376–396.

——— 1961, Elastic inclusions and inhomogeneities, *in* Progress in solid mechanics: I. N. Sneddon and R. Hill, eds., v. 2, p. 89–140.

Hashin, Z., 1962, The elastic moduli of heterogeneous materials: J. Appl. Mech., v. 29E, p. 143–150.

——— 1964, Theory of mechanical behavior of heterogeneous media: Appl. Mech. Rev., v. 17, p. 1–9.

——— 1970, Theory of composite materials: Proc. 5th Sympos. Naval Structural Mech., May 8–10, 1967, New York, Pergamon Press.

Hashin, Z., and Shtrikman, S., 1963, A variational approach to the theory of the elastic behavior of multiphase materials: J. Mech. Phys. Solids, v. 11, p. 127.

Korringa, J., 1973, Theory of elastic constants of heterogeneous media: J. Math. Phys., v. 14, p. 509–513.

Kuster, G. T., 1972, Seismic wave propagation in two-phase media and its application to the earth's interior: Ph.D. thesis, M.I.T., Cambridge.

Kuster, G. T., and Toksöz, M. N., 1974, Velocity and attenuation of seismic waves in two-phase media: Part II. Experimental results: Geophysics, (this issue, p. 607–618.

Lamb, H., 1932, Hydrodynamics: New York, Dover publications.

Mal, A. K., and Knopoff, L., 1967, Elastic wave velocities in two-component systems: J. Inst. Math. Appl., v. 3, p. 376–387.

Morse, P. M., and Feshbach, H., 1953, Methods of theoretical physics: New York, McGraw-Hill Book Co., Inc.

Nur, A., and Simmons, G., 1969, The effect of viscosity of a fluid phase on velocity in low porosity rocks: Earth Plan, Sci. Lett., v. 7, p. 99.

Solomon, S. C., 1971, Seismic wave attenuation and the state of the upper mantle: Ph.D. Thesis, M.I.T., Cambridge.

——— 1972, Seismic wave attenuation and partial melting in the upper mantle of North America: J. Geophys. Res., v. 77, p. 1483–1502.

Takeuchi, S., and Simmons, G., 1973, Elasticity of water-saturated rocks as a function of temperature and pressure: J. Geophys. Res., v. 78, p. 3310–3319.

Timur, A., Hempkins, W. B., and Weinbrandt, R. M., 1971, Scanning electron microscope study of pore

systems in rocks: J. Geophys. Res., v. 76, p. 4932–4948.
Walsh, J. B., 1965, The effect of cracks on the compressibility of rock: J. Geophys. Res., v. 70, p. 381–389.
——— 1969, New analysis of attenuation in partially melted rock: J. Geophys. Res., v. 74, p. 4333–4337.
Wu, T. T., 1966, The effect of inclusion shape on the elastic moduli of a two-phase material: Int. J. Solids and Structures, v. 2, p. 1–8.
Yamakawa, N., 1962, Scattering and attenuation of elastic waves: Geophysical Magazine (Tokyo), v. 31, p. 63–103.
Zeller, R., and Dederichs, P. H., 1973, Elastic constants of polycrystals: Physica Status Solidi (b), v. 55, p. 831–842.

APPENDIX A

Consider a homogeneous and isotropic sphere with elastic constants λ' and μ' and density ρ' embedded in a homogeneous and isotropic infinite matrix with elastic constants λ and μ and density ρ. Let a plane P-wave be incident along the x-axis with displacement

$$u_x = \frac{A}{ip} e^{i(px-\omega t)}, \tag{A-1}$$

where A is the amplitude, p the wavenumber, and ω the angular frequency. The presence of the sphere generates four additional waves: the P- and S-waves inside the sphere and the P- and S-waves scattered into the matrix. We formulate the problem in spherical coordinates with the origin at the center of the sphere (Figure 1). Because of the symmetries of the problem we need not consider the azimuthal dependence. Following Yamakawa (1962), we express the radial and transverse displacements u and v corresponding to each wave in an infinite series of spherical Bessel functions and Legendre polynomials. Thus the incident P-wave components are:

$$\begin{aligned} u_0 &= -\frac{A}{p^2}\sum_{n=0}^{\infty}(2n+1)i^n \frac{d}{dr} j_n(pr)P_n(\cos\theta), \\ v_0 &= -\frac{A}{p^2}\sum_{n=1}^{\infty}(2n+1)i^n \frac{j_n(pr)}{r}\frac{d}{d\theta}P_n(\cos\theta). \end{aligned} \tag{A-2}$$

The scattered P-waves are

$$\begin{aligned} u_1 &= -\frac{1}{p^2}\sum_{n=0}^{\infty} B_n \frac{d}{dr} h_n^{(1)}(pr)P_n(\cos\theta), \\ v_1 &= -\frac{1}{p^2}\sum_{n=1}^{\infty} B_n \frac{h_n^{(1)}(pr)}{r}\frac{d}{d\theta}P_n(\cos\theta). \end{aligned} \tag{A-3}$$

The scattered S-waves are

$$\begin{aligned} u_2 &= -\frac{1}{s^2}\sum_{n=1}^{\infty} C_n n(n+1)\frac{h_n^{(1)}(sr)}{r} P_n(\cos\theta), \\ v_2 &= -\frac{1}{s^2}\sum_{n=1}^{\infty} \frac{C_n}{r}\frac{d}{dr}\left[r h_n^{(1)}(sr)\right]\frac{d}{d\theta}P_n(\cos\theta). \end{aligned} \tag{A-4}$$

The P-waves in the sphere are

$$\begin{aligned} u_3 &= -\frac{1}{p'^2}\sum_{n=0}^{\infty} D_n \frac{d}{dr} j_n(p'r)P_n(\cos\theta), \\ v_3 &= -\frac{1}{p'^2}\sum_{n=1}^{\infty} D_n \frac{j_n(p'r)}{r}\frac{d}{d\theta}P_n(\cos\theta). \end{aligned} \tag{A-5}$$

Downloaded 05/16/13 to 147.188.128.74. Redistribution subject to SEG license or copyright; see Terms of Use at http://library.seg.org/

Downloaded 05/16/13 to 147.188.128.74. Redistribution subject to SEG license or copyright; see Terms of Use at http://library.seg.org/

The S-waves in the sphere are

$$u_1 = -\frac{1}{s'^2}\sum_{n=1}^{\infty} E_n n(n+1)\frac{j_n(s'r)}{r} P_n(\cos\theta),$$
$$v_1 = -\frac{1}{s'^2}\sum_{n=1}^{\infty} \frac{E_n}{r}\frac{d}{dr}\left[rj_n(s'r)\right]\frac{d}{d\theta} P_n(\cos\theta). \tag{A-6}$$

The $e^{-i\omega t}$ time dependence is omitted throughout for brevity, and p and s (p' and s') denote the wavenumbers of P- and S-waves in matrix (inclusion) material. $P_n(\cos\theta)$ is the Legendre polynomial of the nth order, $j_n(z)$ is the spherical Bessel function of the nth order, and $h_n^{(1)}(z)$ is the spherical Hankel function of the first kind and the nth order. We must use $h_n^{(1)}(z)$ for waves traveling radially outward because we adopted an $e^{-i\omega t}$ time dependence. The coefficients in the series are determined from the boundary conditions on the surface of the sphere ($r=a$). The boundary conditions are continuity of the displacements and of the normal stresses

$$\lambda(\Delta_0+\Delta_1)+2\mu\frac{\partial}{\partial r}(u_0+u_1+u_2) = \lambda'\Delta_3+2\mu'\frac{\partial}{\partial r}(u_3+u_4),$$
$$\mu T = \mu' T',$$
$$u_0+u_1+u_2 = u_3+u_4,$$
$$v_0+v_1+v_2 = v_3+v_4, \tag{A-7}$$

where

$$T = \frac{\partial}{\partial r}(v_0+v_1+v_2) - \frac{1}{r}(v_0+v_1+v_2) + \frac{1}{r}\frac{\partial}{\partial\theta}(u_0+u_1+u_2),$$
$$T' = \frac{\partial}{\partial r}(v_3+v_4) - \frac{1}{r}(v_3+v_4) + \frac{1}{r}\frac{\partial}{\partial\theta}(u_3+u_4),$$
$$\Delta_j = \frac{1}{r^2\sin\theta}\left[\frac{\partial}{\partial r}(r^2\sin\theta u_j) + \frac{\partial}{\partial\theta}\left[r\sin\theta v_j\right]\right], \qquad j = 0,\ 1,\text{ or } 3.$$

Putting (A-2) to (A-6) in (A-7), we obtain the following system of four equations with four unknowns for each $n \geq 1$

$$\beta_{n1}B_n+\gamma_{n1}C_n+\delta_{n1}D_n+\epsilon_{n1}E_n = i^n(2n+1)\alpha_{n1}A,$$
$$\beta_{n2}B_n+\gamma_{n2}C_n+\delta_{n2}D_n+\epsilon_{n2}E_n = i^n(2n+1)\alpha_{n2}A,$$
$$\beta_{n3}B_n+\gamma_{n3}C_n+\delta_{n3}D_n+\epsilon_{n3}E_n = i^n(2n+1)\alpha_{n3}A,$$
$$\beta_{n4}B_n+\gamma_{n4}C_n+\delta_{n4}D_n+\epsilon_{n4}E_n = i^n(2n+1)\alpha_{n4}A, \tag{A-8}$$

where

$$\alpha_{n1} = -\left\{\left[(\lambda+2\mu)-\frac{2\mu(n+1)(n+2)}{\xi^2}\right]j_n(\xi)+\frac{4\mu}{\xi}j_{n-1}(\xi)\right\},$$
$$\beta_{n1} = \left[(\lambda+2\mu)-\frac{2\mu(n+1)(n+2)}{\xi^2}\right]h_n^{(1)}(\xi)+\frac{4\mu}{\xi}h_{n-1}^{(1)}(\xi),$$
$$\gamma_{n1} = \frac{-2\mu n(n+1)}{\eta^2}\left[\eta h_{n-1}^{(1)}(\eta)-(n+2)h_n^{(1)}(\eta)\right], \tag{A-9}$$

Downloaded 05/16/13 to 147.188.128.74. Redistribution subject to SEG license or copyright; see Terms of Use at http://library.seg.org/

$$\delta_{n1} = - \left\{\left[(\lambda' + 2\mu') - \frac{2\mu'(n+1)(n+2)}{\xi'^2}\right] j_n(\xi') + \frac{4\mu'}{\xi'} j_{n-1}(\xi')\right\},$$

$$\epsilon_{n1} = \frac{2\mu' n(n+1)}{\eta'^2} \left[\eta' j_{n-1}(\eta') - (n+2) j_n(\eta')\right],$$

$$\alpha_{n2} = -\frac{2\mu}{\xi^2}\left[(n+2) j_n(\xi) - \xi j_{n-1}(\xi)\right],$$

$$\beta_{n2} = \frac{2\mu}{\xi^2}\left[(n+2) h_n^{(1)}(\xi) - \xi h_{n-1}^{(1)}(\xi)\right],$$

$$\gamma_{n2} = \frac{\mu}{\eta^2}\left\{2\eta h_{n-1}^{(1)}(\eta) + \left[\eta^2 - 2n(n+2)\right] h_n^{(1)}(\eta)\right\}, \tag{A-10}$$

$$\delta_{n2} = -\frac{2\mu'}{\xi'^2}\left[(n+2) j_n(\xi') - \xi' j_{n-1}(\xi')\right],$$

$$\epsilon_{n2} = -\frac{\mu'}{\eta'^2}\left\{2\eta' j_{n-1}(\eta') + \left[\eta'^2 - 2n(n+2)\right] j_n(\eta')\right\},$$

$$\alpha_{n3} = \frac{1}{\xi}\left[j_{n-1}(\xi) - \frac{n+1}{\xi} j_n(\xi)\right], \qquad \gamma_{n3} = -\frac{n(n+1)}{\eta^2} h_n^{(1)}(\eta),$$

$$\beta_{n3} = -\frac{1}{\xi}\left[h_{n-1}^{(1)}(\xi) - \frac{n+1}{\xi} h_n^{(1)}(\xi)\right], \qquad \delta_{n3} = \frac{1}{\xi'}\left[j_{n-1}(\xi') - \frac{n+1}{\xi'} j_n(\xi')\right], \tag{A-11}$$

$$\epsilon_{n3} = \frac{n(n+1)}{\eta'^2} j_n(\eta'),$$

and

$$\alpha_{n4} = \frac{1}{\xi^2} j_n(\xi), \qquad \gamma_{n4} = -\frac{1}{\eta^2}\left[\eta h_{n-1}^{(1)}(\eta) - n h_n^{(1)}(\eta)\right],$$

$$\beta_{n4} = -\frac{1}{\xi^2} h_n^{(1)}(\xi), \qquad \delta_{n4} = \frac{1}{\xi'^2} j_n(\xi'), \tag{A-12}$$

$$\epsilon_{n4} = \frac{1}{\eta'^2}\left[\eta' j_{n-1}(\eta') - n j_n(\eta')\right],$$

with

$$\xi = pa, \qquad \eta = sa, \qquad \xi' = p'a, \qquad \eta' = s'a.$$

For $n=0$, equation (A-8) can be written as

$$\beta_{01} B_0 + \delta_{01} D_0 = \alpha_{01} A, \qquad \beta_{03} B_0 + \delta_{03} D_0 = \alpha_{03} A, \tag{A-13}$$

where

$$\alpha_{01} = -\left[(\lambda + 2\mu) j_0(\xi) - \frac{4\mu}{\xi} j_1(\xi)\right],$$

$$\beta_{01} = \left[(\lambda + 2\mu) h_0^{(1)}(\xi) - \frac{4\mu}{\xi} h_1^{(1)}(\xi) \right], \tag{A-14}$$

$$\delta_{01} = - \left[(\lambda' + 2\mu') j_0(\xi') - \frac{4\mu'}{\xi'} j_1(\xi') \right],$$

and

$$\alpha_{03} = -\frac{1}{\xi} j_1(\xi), \qquad \beta_{03} = \frac{1}{\xi} h_1^{(1)}(\xi), \qquad \delta_{03} = -\frac{1}{\xi'} j_1(\xi'). \tag{A-15}$$

Cramer's rule can be used to solve systems (A-8) and (A-13) for the coefficients in the series expansions of the scattered waves. When the wavelengths of *all* waves are much longer than the radius of the sphere (ξ, ξ', η, η' much smaller than 1), we may use the expansions of the spherical Bessel and Hankel functions for small arguments. They are, for $z \ll 1$,

$$j_n(z) \simeq \frac{2^r n!}{(2n+1)!} z^n \left[1 - \frac{z^2}{2(2n+3)} \right],$$

$$h_0^{(1)}(z) \simeq -\frac{i}{z}(1 + iz), \tag{A-16}$$

$$h_n^{(1)}(z) \simeq -\frac{i(2n)!}{2^n n! z^{n+1}} \left[1 + \frac{z^2}{2(2n-1)} \right] \qquad \text{for } n \geq 1.$$

Using the expansions in (A-9) to (A-12), (A-14) and (A-15), and keeping only the dominant term in solving systems (A-8) and (A-13), we obtain

$$B_0 = Ai\xi^3 \frac{K - K'}{3K' + 4\mu}, \tag{A-17}$$

$$B_1 = \frac{A\xi^3}{3} \frac{(\rho - \rho')}{\rho}, \tag{A-18}$$

$$B_2 = \frac{20iA\xi^3}{3} \frac{\mu(\mu' - \mu)}{6\mu'(K + 2\mu) + \mu(9K + 8\mu)}, \tag{A-19}$$

$$B_n \simeq -i^{n+1} A F_n \xi^{2n-1} \frac{\mu(\mu' - \mu)}{\left[\begin{array}{l} 2(n+1)(n-1)K\mu' + (2n^2+1)K\mu \\ \quad + \frac{2}{3}(n-1)(7n+4)\mu\mu' + \frac{2}{3}(n+1)(n+2)\mu^2 \end{array} \right]} \tag{A-20}$$

for $n \geq 3$,

$$C_n = \left(\frac{s}{p} \right)^{n+3} \frac{B_n}{n} \qquad \text{for } n \geq 1, \tag{A-21}$$

where

$$F_n = 2n(n-1)(2n+1)(2n-1) \left[\frac{2^n n!}{(2n)!} \right]^2, \qquad K = \lambda + \tfrac{2}{3}\mu, \qquad K' = \lambda' + \tfrac{2}{3}\mu'.$$

For an observation point at a large distance from the sphere ($pr \gg 1$, $sr \gg 1$), we may use the asymptotic expansion of the Hankel function

Downloaded 05/16/13 to 147.188.128.74. Redistribution subject to SEG license or copyright; see Terms of Use at http://library.seg.org/

$$h_n^{(1)}(z) \simeq (-i)^{n+1}\frac{e^{iz}}{z} \qquad \text{for } z \gg 1, \tag{A-22}$$

and we may thus write the scattered P-waves as

$$\begin{aligned} u_1 &= -\frac{1}{p^2}\frac{e^{ipr}}{r}\sum_{n=0}^{\infty}(-i)^n B_n P_n(\cos\theta), \\ v_1 &= -\frac{1}{p^2}\frac{e^{ipr}}{pr^2}\sum_{n=1}^{\infty}(-i)^{n+1}B_n\frac{d}{d\theta}P_n(\cos\theta), \end{aligned} \tag{A-23}$$

and the scattered S-waves as

$$\begin{aligned} u_2 &= -\frac{1}{s^2}\frac{e^{isr}}{sr^2}\sum_{n=1}^{\infty}n(n+1)(-i)^{n+1}C_n P_n(\cos\theta), \\ v_2 &= -\frac{1}{s^2}\frac{e^{isr}}{r}\sum_{n=1}^{\infty}(-i)^n C_n\frac{d}{d\theta}P_n(\cos\theta). \end{aligned} \tag{A-24}$$

Since $pr \gg 1$ and $sr \gg 1$, v_1 can be neglected with respect to u_1, and u_2 can be neglected with respect to v_2. Furthermore, in the long wavelength case all coefficients for $n \geq 3$ are of higher order than the leading coefficients. Thus, keeping only the dominant terms, we can write the scattered waves as

$$\begin{aligned} u &= -\frac{iA}{p}(pa)^3\frac{e^{i(pr-\omega t)}}{pr}\left[Be_0 - Be_1\cos\theta - \frac{Be_2}{4}(3\cos 2\theta + 1)\right], \\ v &= -iA\frac{(sa)^3}{p}\frac{e^{i(sr-\omega t)}}{sr}\left[Be_1\sin\theta + \frac{3s}{4p}Be_2\sin 2\theta\right], \end{aligned} \tag{A-25}$$

where

$$Be_0 = \frac{K - K'}{3K' + 4\mu}, \qquad Be_1 = \frac{\rho - \rho'}{3\rho}, \qquad Be_2 = \frac{20}{3}\,\frac{\mu(\mu' - \mu)}{6\mu'(K + 2\mu) + \mu(9K + 8\mu)}\,. \tag{A-26}$$

The neglected terms are of order $(pa)^5$.

When the matrix is a nonviscous fluid, there are no scattered S-waves and the continuity of the transverse displacement at the boundary is not required. Thus, the coefficients in the expansion of the scattered P-waves are the solutions of the following systems.

For $n = 0$

$$\overset{0}{\beta}_{01}B_0 + \delta_{01}D_0 = \overset{0}{\alpha}_{01}A, \qquad \beta_{03}B_0 + \delta_{03}D_0 = \overset{0}{\alpha}_{03}A. \tag{A-27}$$

For $n \geq 1$

$$\begin{aligned} \overset{0}{\beta}_{n1}B_n + \delta_{n1}D_n + \epsilon_{n1}E_n &= (2n+1)i^n\overset{0}{\alpha}_{n1}A, \\ \overset{0}{\beta}_{n2}B_n + \delta_{n2}D_n + \epsilon_{n2}E_n &= (2n+1)i^n\overset{0}{\alpha}_{n2}A, \\ \overset{0}{\beta}_{n3}B_n + \delta_{n3}D_n + \epsilon_{n3}E_n &= (2n+1)i^n\overset{0}{\alpha}_{n3}A. \end{aligned} \tag{A-28}$$

The coefficients δ_{nm} and ϵ_{nm} are the same as in (A-9) to (A-11), whereas β_{nm}^0 and α_{nm}^0 are obtained from

Downloaded 05/16/13 to 147.188.128.74. Redistribution subject to SEG license or copyright; see Terms of Use at http://library.seg.org/

Downloaded 05/16/13 to 147.188.128.74. Redistribution subject to SEG license or copyright; see Terms of Use at http://library.seg.org/

β_{nm} and α_{nm} in (A-9) to (A-11) by letting μ vanish. The calculation is now similar to that of the preceding section. In the long wavelength approximation (ξ, ξ' and η' much smaller than 1) and for an observation point at a large distance from the sphere ($pr \gg 1$), the scattered waves can be written as

$$u = -\frac{iA(pa)^3}{p}\frac{e^{i(pr-\omega t)}}{pr}\left[B\overset{0}{e}_0 - B\overset{0}{e}_1 \cos\theta\right], \tag{A-29}$$

where

$$B\overset{0}{e}_0 = \frac{K - K'}{3K'}; \qquad B\overset{0}{e}_1 = \frac{\rho - \rho'}{\rho + 2\rho'}. \tag{A-30}$$

The terms neglected are of order $(pa)^5$.

APPENDIX B

To find the waves scattered by a spheroidal inclusion embedded in a solid matrix, we shall use an integral expression derived by Mal and Knopoff (1967) for the displacement due to the waves scattered by an inclusion of arbitrary shape isolated in an infinite matrix. Denoting the displacement field of the scattered waves observed at a point $\mathbf{x}$ in the matrix by $\Delta\mathbf{u}(\mathbf{x})$, the displacement field of the wave at a point $\boldsymbol{\xi}$ inside the inclusion by $\mathbf{v}(\boldsymbol{\xi})$, the kth component of the Green's function due to a point force acting in the ith direction at a point $\mathbf{y}$ in the infinite matrix by $G_{ki}(\mathbf{x}, \mathbf{y})$, and the elastic sensor in the matrix by c_{ijpq}, we have

$$\Delta u_k(\mathbf{x}) = \int_V \left\{\omega^2(\rho' - \rho)v_i(\boldsymbol{\xi})G_{ki}(\mathbf{x}, \boldsymbol{\xi}) - (c'_{ijpq} - c_{ijpq})\frac{\partial v_p}{\partial \xi_q}\frac{\partial G_{ki}}{\partial \xi_j}(\mathbf{x}, \boldsymbol{\xi})\right\} d\boldsymbol{\xi}. \tag{B-1}$$

The summation convention is used and we omit, for brevity, the assumed $e^{i\omega t}$ time dependence. The integral is taken over the volume V of the inclusion. If the displacement and strain inside the inclusion can be estimated in terms of the incident field, we can obtain the desired expression for the scattered field.

When the matrix is solid, and the wavelengths are much longer than the inclusion size, the lowest order approximation (known as the Born approximation) to the displacement inside is the displacement one would observe if the inclusion were absent (Mal and Knopoff, 1967). In other words, we may write

$$\mathbf{v}(\boldsymbol{\xi}) \simeq \mathbf{u}^0(\boldsymbol{\zeta}), \tag{B-2}$$

where $\boldsymbol{\zeta}$ is the center of the inclusion. No assumption about the shape of the inclusion is required so that we can use (B-2) for a spheroidal inclusion.

Mal and Knopoff (1967) showed that for arbitrary contrast between the elastic properties, the lowest order approximation to the strain inside a *spherical* inclusion in terms of the incident strain is given by

$$e_{kl}(\boldsymbol{\zeta}) = \tfrac{1}{3}(P - Q)\overset{0}{e}_{ii}(\boldsymbol{\zeta})\delta_{kl} + Q\overset{0}{e}_{kl}(\boldsymbol{\zeta}), \tag{B-3}$$

where δ_{kl} is a Kronecker delta and

$$P = \frac{3K + 4\mu}{3K' + 4\mu}, \qquad Q = \frac{5\mu(3K + 4\mu)}{6\mu'(K + 2\mu) + \mu(9K + 8\mu)}. \tag{B-4}$$

The important feature of this result is that it is the same as that obtained by Eshelby (1957) for the static strain inside a sphere when a uniform strain is applied at infinity. Thus, for a spherical inclusion and for waves of long wavelengths, the lowest order approximation is given by the solution of the corresponding static problem. We *assume* this identity also holds for a spheroidal inclusion. The expression derived by Eshelby (1957), for the strain inside a spheroid of arbitrary orientation with respect to the fixed coordinate system of the matrix, is

$$e_{ij} = U_{ijkl}\overset{0}{e}_{kl}, \tag{B-5}$$

where

$$U_{ijkl} = l_{\alpha i}l_{\beta j}l_{\gamma k}l_{\delta l}T_{\alpha\beta\gamma\delta}.$$

The l_{mn} are direction cosines, and $T_{\alpha\beta\gamma\delta}$ is a fourth order tensor which is described later in this Appendix.

Introducing (B-2) and (B-5) in (B-1) and using

$$c_{ijpq} = \lambda\delta_{ij}\delta_{pq} + \mu(\delta_{ip}\delta_{jq} + \delta_{iq}\delta_{jp}), \tag{B-6}$$

we obtain

$$\begin{aligned}\Delta u_k(\mathbf{x}, \boldsymbol{\zeta}) &= \omega^2(\rho' - \rho)\overset{0}{u}_i(\boldsymbol{\zeta}) \int_V G_{ki}(\mathbf{x}, \boldsymbol{\xi})d\boldsymbol{\xi} \\ &\quad - [(\lambda' - \lambda)U_{pprs}\delta_{ij} + 2(\mu' - \mu)U_{ijrs}]\overset{0}{e}_{rs} \int_V \frac{\partial G_{ki}}{\partial \xi_j}(\mathbf{x}, \boldsymbol{\xi})d\boldsymbol{\xi}.\end{aligned} \tag{B-7}$$

The integrals of the Green's function over the volume of the spheroid can be evaluated easily when the point of observation is at a great distance from the spheroid. With this condition we have

$$\int_V G_{ki}(\mathbf{x}, \boldsymbol{\xi})d\boldsymbol{\xi} \simeq VG_{ki}(\mathbf{x}, \boldsymbol{\zeta}). \tag{B-8}$$

Finally, by using (B-8) and the symmetry of the Green's function, we can write the displacement field scattered by a spheroid of arbitrary orientation as

$$\begin{aligned}\Delta u_k(\mathbf{x}, \boldsymbol{\zeta}) = V\Big[&\omega^2(\rho' - \rho)\overset{0}{u}_i(\boldsymbol{\zeta})G_{ki}(\mathbf{x}, \boldsymbol{\zeta}) \\ &- [(\lambda' - \lambda)U_{pprs}\delta_{ij} + 2(\mu' - \mu)U_{ijrs}]\overset{0}{e}_{rs} \frac{\partial G_{ki}}{\partial \zeta_j}(\mathbf{x}, \boldsymbol{\zeta})\Big].\end{aligned} \tag{B-9}$$

$T_{\alpha\beta\gamma\delta}$ is a fourth order tensor whose symmetries for an oblate spheroid with aspect ratio α are

$$\begin{aligned} &T_{1111} = T_{2222}, \qquad T_{1133} = T_{2233}, \\ &T_{1122} = T_{2211}, \qquad T_{3322} = T_{3311}, \\ &T_{1212} = T_{1221} = T_{2121} = T_{2112}, \\ &T_{1313} = T_{1331} = T_{3113} = T_{3131}, \\ &T_{2323} = T_{2332} = T_{3223} = T_{3232}. \end{aligned} \tag{B-10}$$

We also have the relation

$$T_{1111} - T_{1122} - 2T_{1212} = 0. \tag{B-11}$$

Downloaded 05/16/13 to 147.188.128.74. Redistribution subject to SEG license or copyright; see Terms of Use at http://library.seg.org/

The scalars T_{iijj} and T_{ijij} which are used in the text are given by

$$T_{iijj} = -\frac{3F_1}{F_2},$$

$$T_{ijij} - \frac{1}{3}T_{iijj} = \frac{2}{F_3} + \frac{1}{F_4} + \frac{F_4F_5 + F_6F_7 - F_8F_9}{F_2F_4}, \qquad \text{(B-12)}$$

where

$$F_1 = 1 + A\left[\frac{3}{2}(g+\phi) - R\left(\frac{3}{2}g + \frac{5}{2}\phi - \frac{4}{3}\right)\right],$$

$$F_2 = 1 + A\left[1 + \frac{3}{2}(g+\phi) - \frac{R}{2}(3g+5\phi)\right] + B(3-4R)$$
$$+ \frac{A}{2}(A+3B)(3-4R)[g + \phi - R(g - \phi + 2\phi^2)],$$

$$F_3 = 1 + \frac{A}{2}\left[R(2-\phi) + \frac{(1+\alpha^2)}{\alpha^2}g(R-1)\right],$$

$$F_4 = 1 + \frac{A}{4}[3\phi + g - R(g-\phi)],$$

$$F_5 = A\left[R\left(g + \phi - \frac{4}{3}\right) - g\right] + B\phi(3-4R),$$

$$F_6 = 1 + A[1 + g - R(g+\phi)] + B(1-\phi)(3-4R),$$

$$F_7 = 2 + \frac{A}{4}[9\phi + 3g - R(5\phi + 3g)] + B\phi(3-4R),$$

$$F_8 = A\left[1 - 2R + \frac{g}{2}(R-1) + \frac{\phi}{2}(5R-3)\right] + B(1-\phi)(3-4R),$$

$$F_9 = A[g(R-1) - R\phi] + B\phi(3-4R).$$

$$A = \frac{\mu'}{\mu} - 1, \qquad B = \frac{1}{3}\left(\frac{K'}{K} - \frac{\mu'}{\mu}\right), \qquad R = \frac{3\mu}{3K + 4\mu},$$

$$\phi = \frac{\alpha}{(1-\alpha^2)^{3/2}}[\cos^{-1}\alpha - \alpha(1-\alpha^2)^{1/2}], \qquad g = \frac{\alpha^2}{1-\alpha^2}(3\phi - 2).$$

Downloaded 05/16/13 to 147.188.128.74. Redistribution subject to SEG license or copyright; see Terms of Use at http://library.seg.org/